We are IntechOpen, the world's leading publisher of Open Access books Built by scientists, for scientists

6,900
Open access books available

185,000
International authors and editors

200M
Downloads

Our authors are among the

154
Countries delivered to

TOP 1%
most cited scientists

12.2%
Contributors from top 500 universities



WEB OF SCIENCE™

Selection of our books indexed in the Book Citation Index in Web of Science™ Core Collection (BKCI)

Interested in publishing with us?
Contact book.department@intechopen.com

Numbers displayed above are based on latest data collected.
For more information visit www.intechopen.com



Provisional chapter

Thermal Stability and Mechanical Properties of Extruded Mg-Zn-Y Alloys with a Long-Period Stacking Order Phase and Plastic Deformation

Masafumi Noda1, Kunio Funami1,
Yoshihito Kawamura2 and Tsuyoshi Mayama2

Additional information is available at the end of the chapter

http://dx.doi.org/10.5772/48202

1. Introduction

Lightweight Mg alloys with excellent shock-absorption properties are being actively adopted for use in electronic information devices and automotive parts [1]. For such structural applications, Mg alloys need to have adequate ductility, thermal stability, and strength. However, Mg alloys often exhibit low ductility and low tensile yield strength at room temperature and above as a result of a scarcity of slip systems in their hexagonal close-packed structures [2]. Effective ways of improving the ductility and tensile yield strength of Mg alloys include grain refinement [3] and control of the texture [4]; these techniques promote prismatic slips and facilitate the creation of large plastic deformations. Recently, alloys of Mg with transition metals (TMs), such as Co, Ni, Cu, or Zn, and rare-earth (RE) metals, such as Y, Gd, Tb, Dy, Ho, or Er, have been found to show superior mechanical properties to those of other Mg alloys [5,6]. A characteristic of these Mg–TM–RE alloy systems is the formation of a long-period stacking order (LPSO) phase in as-cast materials and/or after heat treatment. In the present study, we examined the annealing properties, tensile properties, thermal stability, and rolling workability of high-strength extruded $Mg_{96}Zn_2Y_2$ alloys.

$Mg_{96}Zn_2Y_2$ alloy contains an LPSO phase as a secondary phase in the dominant α-Mg phase [5,6]. In general, Mg alloys with LPSO phases are known to have greatly enhanced mechanical properties, whereas their ductility can be maintained only by extrusion and/or plastic deformation treatments of the cast metal. It has been suggested that kink deformations in the LPSO phase and microstructural refinement in the α-Mg phase occur during extrusion deformation [7]. The tensile yield strength, microstructure, fatigue properties, and thermal sta-

INTECH
open science | open minds

© 2012 Noda et al.; licensee InTech. This is an open access article distributed under the terms of the Creative Commons Attribution License (http://creativecommons.org/licenses/by/3.0), which permits unrestricted use, distribution, and reproduction in any medium, provided the original work is properly cited.

bility of extruded $Mg_{96}Zn_2Y_2$ and LPSO-type Mg alloy have been reported [8–10]. Enhancements in the strength of $Mg_{96}Zn_2Y_2$ alloy by means of extrusion have been investigated and reported by Kawamura *et al.* [6–7]. However, improvements in ductility, which are vital for industrial application of Mg alloys, have not been investigated in relation to the annealing properties and thermal stability of Mg–Zn–Y alloys. It was therefore necessary to investigate the relationship between changes in the microstructure of the α-Mg and LPSO phases and the reduction in strength and the improvement in ductility produced by annealing of the alloy. Although LPSO-type Mg alloys have a high strength, they also need to display good ductility and high thermal stability before they can find practical industrial applications. In the present study, we examined the effects of various annealing treatments on the microstructure, tensile yield strength, ductility, and thermal stability of samples of $Mg_{96}Zn_2Y_2$ alloy produced by extrusion at 623 K. Annealing was accomplished by holding the extruded sample for 1 to 100 h in an electric furnace at various temperatures between 473 and 773 K.

Additionally, many of the plastic deformation processes of LPSO-type Mg alloy and other high-strength materials are affected by extrusion processing and there have been few attempts to examine the development of high strength by rolling and other working processes. It is generally known that plastic deformation of Mg alloys containing added RE elements requires many working cycles and a high deformation temperature in comparison with commercial Mg alloys [6,11]. The use of wrought metals as industrial materials is important and, to reduce costs, it is desirable to use plastic-deformation as well as extrusion in processing the materials. In the case of Mg alloys, the establishment of a plastic deformation process that combines a heat-treatment process, a plastic-working process, and controlled microstructures, leading to a reduction in processing costs, is urgently required. We produced a time–temperature–transformation (*TTT*) diagram for $Mg_{96}Zn_2Y_2$ alloys by investigating the microstructure, strength, elongation, and thermal stability of as-extruded and annealed samples at room temperature and at high temperatures. As a result, we succeeded in producing high-strength rolled sheet of $Mg_{96}Zn_2Y_2$ by a few passes of a rolling processing to control the amounts of LPSO phase and α-Mg phase. The fine-grained α-Mg phase did contribute to plastic deformation, but the grain size in the rolled sheet was 5 μm, suggesting that the LPSO phase was responsible for flexible workability as a result of the presence of continuous bending and kink bands at the boundary between the two phases.

2. Experimental procedures

The alloys used in this study were extruded specimens of $Mg_{96}Zn_2Y_2$ (atomic %) alloys. Ingots were prepared by high-frequency induction melting in an Ar atmosphere. A 60-mm-long cast sample with a diameter 29 mm was prepared. This $Mg_{96}Zn_2Y_2$ ingot was extruded at 623 K at an extrusion ratio of 10 and an extrusion speed of 2.5 mms^{-1}. The $Mg_{96}Zn_2Y_2$ alloy consisted of an α-Mg phase, an LPSO phase, and inclusions of $Mg_3Zn_3Y_2$ compounds, with the α-Mg and LPSO phases as the major phases. Samples for tensile testing with gauge sections 2.5 mm in width and 15 mm in length were machined in the direction parallel to the

http://dx.doi.org/10.5772/48202

direction of extrusion from samples of material that had been extruded and annealed. Tensile tests were carried out at an initial strain rate of 5.0×10^{-4} s^{-1} at temperatures between room temperature and 573 K. Hardness tests were carried out for 20 s at a load of 1.96 kN on a plane normal to the direction of extrusion by using a Vickers hardness testing machine. Annealing was carried out at temperatures between 473 and 773 K in an electric furnace for various times between 1 and 100 h, with a maximum holding time of 1000 h, and the specimens were subsequently cooled in water. The microstructures of the extruded and annealed samples were observed by optical microscopy (OM), scanning electron microscopy (SEM), transmission electron microscopy (TEM), and electron backscattering diffraction (EBSD). Samples for microscopy were prepared by using a section polisher. In this study, cross-sections of the microstructure were observed from the direction of the extrusion axis. The SEM micrographs of cast and extruded materials are shown in Figure 1. These micrographs were recorded on cross-sectional planes perpendicular to the direction of extrusion. The brighter areas in Figure 1 correspond to the LPSO phase. The LPSO phase appears to be more finely distributed in the extruded alloys than in the as-cast alloys. The remaining 30% of the α-Mg phase region consisted of a nonrecrystallized material. The volume fraction of the LPSO phase was about 25%.

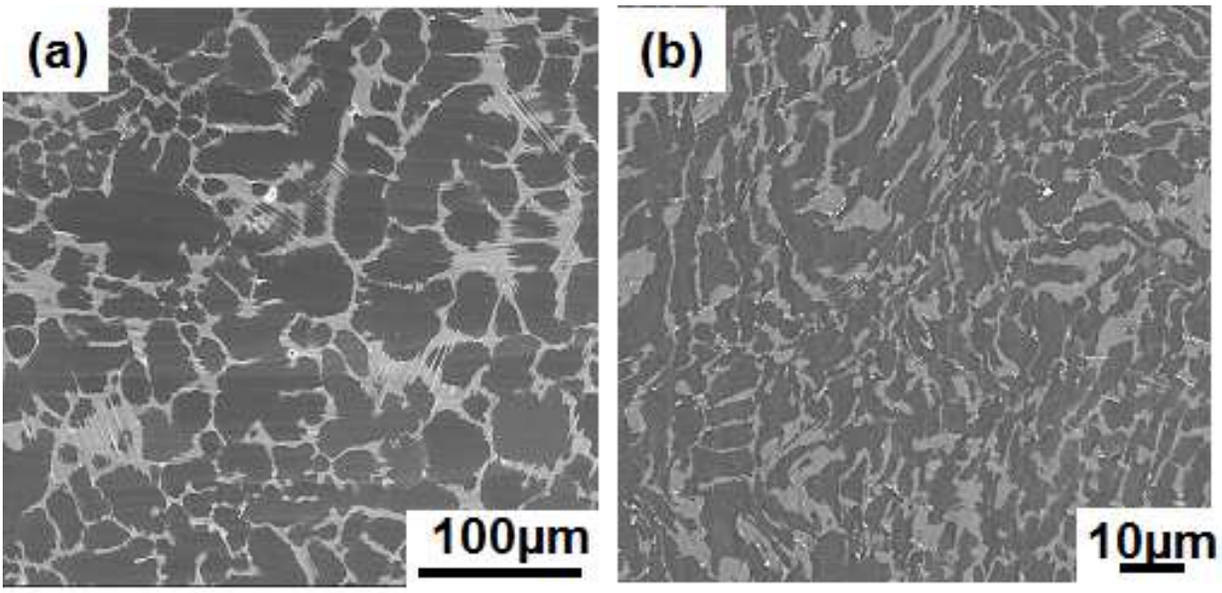


Figure 1. SEM micrographs of cast and extruded samples of $Mg_{96}Zn_2Y_2$ alloy.

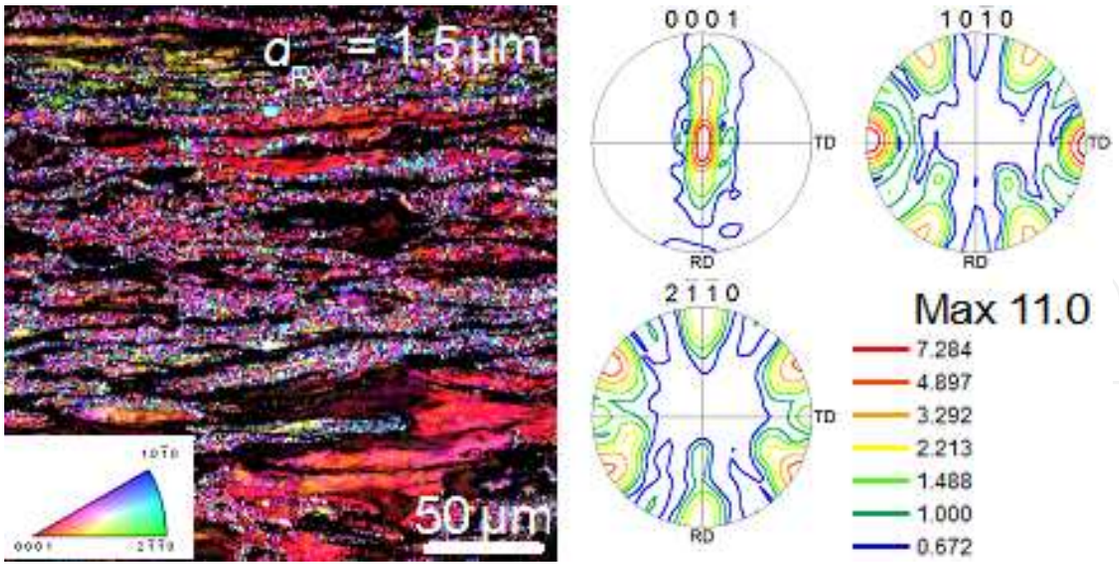


Figure 2. IPF and PF maps of as-extruded samples of $Mg_{96}Zn_2Y_2$. These maps were determined by EBSD, and the intensity of texture is indicated in the PF map.

After we had investigated the microstructure and tensile properties of the as-extruded and annealed materials at room temperature and at high temperatures, we investigated the hot-rolling workability of the material to elucidate the effect of the α-Mg phase and the LPSO phase on the plastic deformability of the $Mg_{96}Zn_2Y_2$ alloy.

In the rolling process, we used extruded $Mg_{96}Zn_2Y_2$ alloy in the form of the as-received material. The α-Mg phase showed static recrystallization grain growth. Kink bands in the LPSO phase were restored by the annealing treatment. Samples 5-mm thick, 20-mm wide, and 50-mm long were machined from the annealed and extruded materials and subjected to rolling in the direction perpendicular to the direction of extrusion. The rolling process was performed at a roll temperature of 473 K and a roll speed of 0.17 m s^{-1}. The sample was subsequently heated at 643 K for 5 min in an electric furnace and, finally, the rolled samples were quenched in water. Tensile samples with a gauge section 2.5 mm in width, 1 mm in thickness, and 12 mm in length were machined in the direction parallel to the rolling direction from the rolled sheet and from the various annealed sheets. In the as-rolled sheet, the cross section of the microstructure was observed from the rolling direction. The methods used to investigate the microstructures and tensile properties of as-rolled $Mg_{96}Zn_2Y_2$ alloy were the same as those used for the extruded and annealed $Mg_{96}Zn_2Y_2$ alloys.

3. Results and discussion

3.1. Tensile properties at room temperature and at high temperatures of extruded and annealed samples of $Mg_{96}Zn_2Y_2$ alloy

The results of tensile tests performed at room temperature and at high temperatures on extruded $Mg_{96}Zn_2Y_2$ samples annealed at various temperatures with holding times of 1 h and

http://dx.doi.org/10.5772/48202

100 h are shown in Figure 3. The yield stress and the tensile strength of the as-extruded sample were 391 and 432 MPa, respectively, and its elongation was 5.4% at room temperature. When the sample was annealed at 623 K for 1 h, the yield stress was 380 MPa and the tensile strength was 410 MPa; annealing at higher temperatures, resulted in a gradual decrease in strength. Even when the annealing time was extended to 100 h, the same tendency of showing a gradual decrease in these properties was observed. In other words, the α-Mg phase undergoes a static recrystallization at 623 K. On the other hand, it is known that the LPSO phase is responsible for local recovery and/or static recrystallization at an annealing temperature of 673 K [10]. At an annealing temperature at 673 K, the strength deteriorated as a result of recovery of kink bands in the LPSO phase and grain growth of the α-Mg phase, but the elongation improved. It has been reported that annealing of conventional Mg alloys at 523 K for 1 h disrupts the crystalline orientation and causes a reduction in strength [12]. Therefore, in comparison with conventional Mg alloy, the ductility of $Mg_{96}Zn_2Y_2$ alloy can be improved while maintaining a high strength, despite the fact that $Mg_{96}Zn_2Y_2$ has a low ductility at room temperature. The hardness of the samples, the mean grain size of the α-Mg phase, and the size of the $Mg_3Zn_3Y_2$ compounds are shown in Figure 4 for each annealing temperature.

As in the case of tensile tests, annealing at 623 K caused almost no reduction in hardness, which fell from HV 101 before annealing to HV 100 after annealing. The mean grain size was 1.5 μm in the as-extruded sample, which still contained nonrecrystallized regions. On the other hands, in the extruded sample annealed at 623 K, the mean grain size was 2.5 μm owing to the recovery of recrystallized and nonrecrystallized regions or to static recrystallization, and the average size of inclusions of $Mg_3Zn_3Y_2$ compound was 0.4 μm. From Figures 3 and 4, the static recrystallization temperature of the α-Mg phase of this alloy was estimated to be 623 K or higher. When the alloy was annealed at 773 K, its yield stress and tensile strength fell to 210 and 320 MPa, respectively, and the hardness was HV 75, whereas the elongation was improved to 23%.

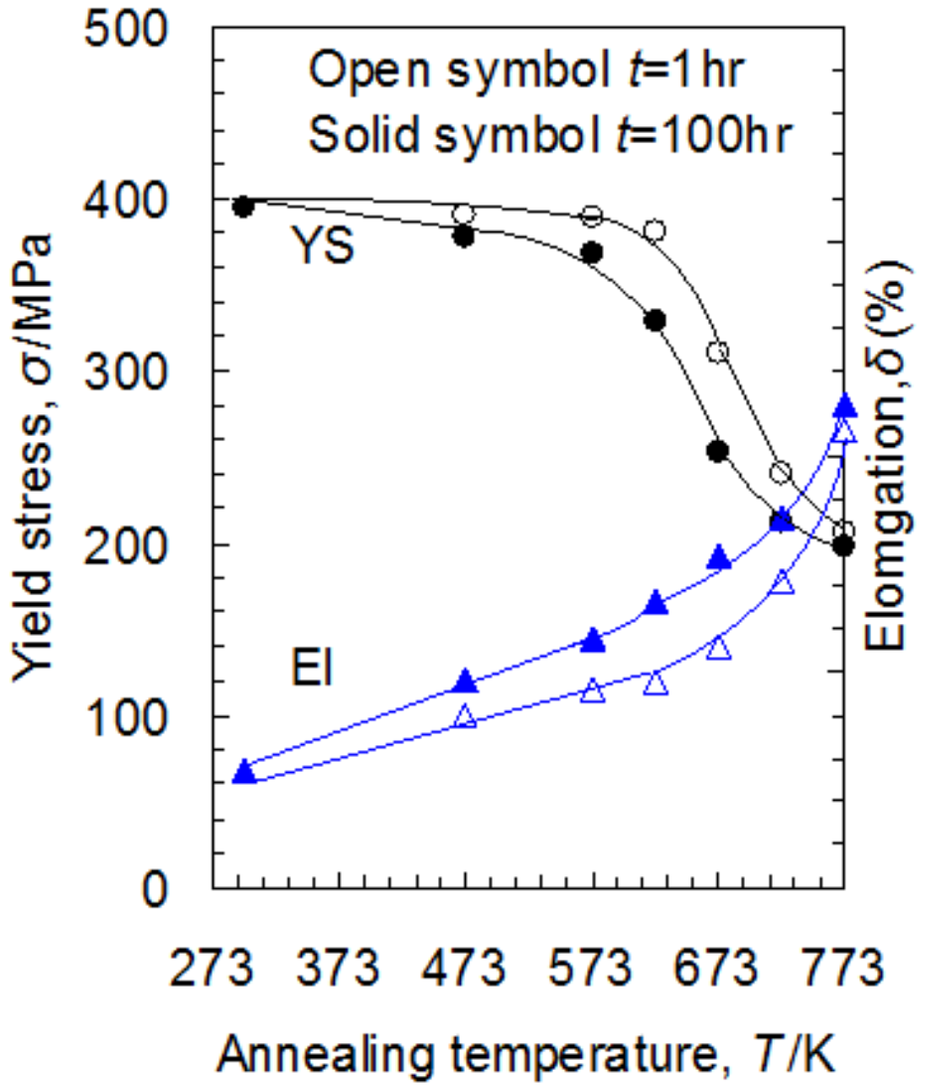


Figure 3. Mechanical properties of extruded and annealed samples of extruded samples of $Mg_{96}Zn_2Y_2$ alloy. Test temperatures: room temperature and 523 K; initial strain rate: 5.0×10^{-4} s^{-1}. T: testing temperature; T_a: annealing temperature; t_a: annealing time.

http://dx.doi.org/10.5772/48202

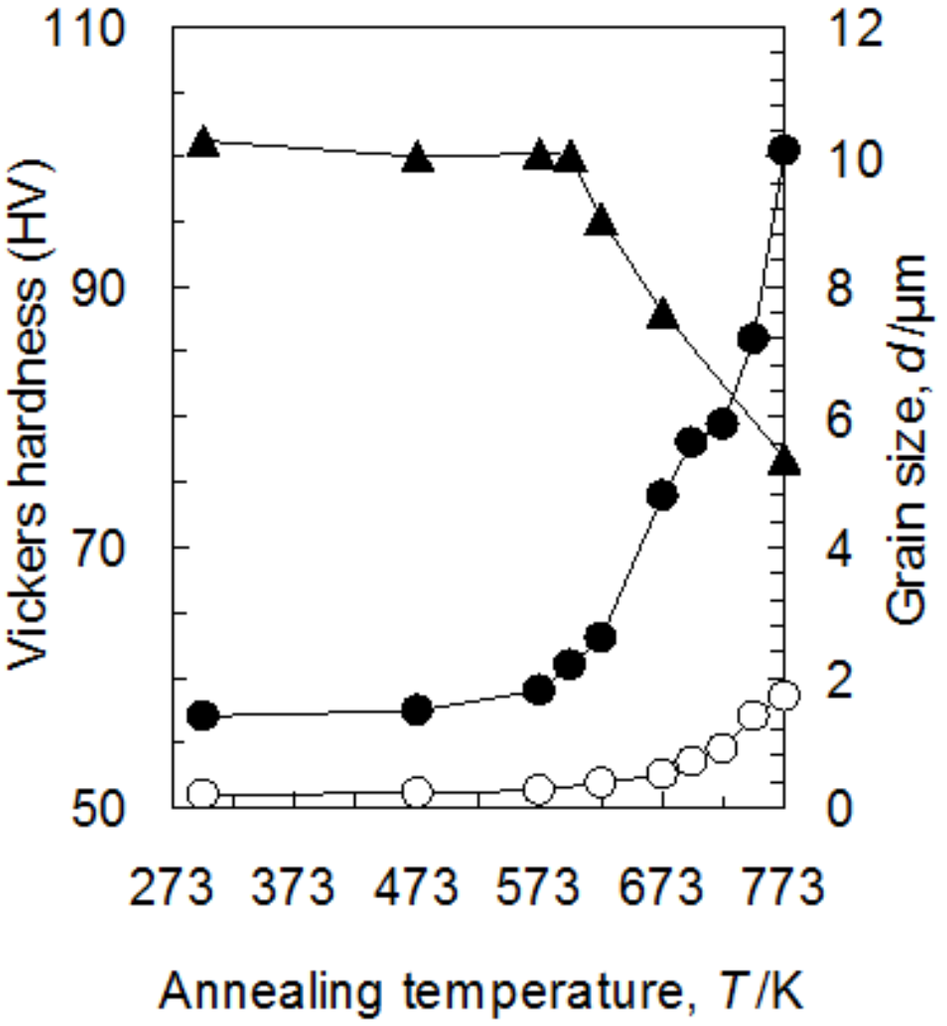


Figure 4. Changes in the hardness, recrystallized grain size of the α-Mg phase, and size of $Mg_3Zn_3Y_2$ phase caused by annealing.

The mean grain size of the α-Mg phase was about 10 μm, and the size of the inclusions of $Mg_3Zn_3Y_2$ compound was 1.7 μm. Fine-grained AZ31 Mg alloy annealed at 773 K for 1 h has a yield stress of 50 MPa, a mean grain size as large as 20 μm, and an improved elongation of 15% [13]. The alloy investigated in the present study showed even better mechanical properties. This was probably because the LPSO phases were dispersed within the α-Mg phase (even at 773 K), the mean grain size of the α-Mg phase was only about 10 μm, and the size of inclusions of $Mg_3Zn_3Y_2$ compound remained small. This tendency persisted when the annealing time was extended from 1 to 100 h, as demonstrated by the microstructural and tensile properties of the samples annealed for 100 h (see Section 3.2). We also carried out high-temperature tensile tests to investigate the temperature dependence of the properties of as-extruded and annealed $Mg_{96}Zn_2Y_2$ alloys; the results of these tests are shown in Figure 5. The tests were performed at 423 to 523 K at an initial strain rate of 5×10^{-4} s^{-1}. The yield

stress and tensile strength of the as-extruded sample were 281 and 307 MPa, respectively, and the elongation was 24% at 523 K. The yield stress and elongation of extruded $Mg_{96}Zn_2Y_2$ alloy depended on the testing temperature, and the yield stress decreased with increasing testing temperature.

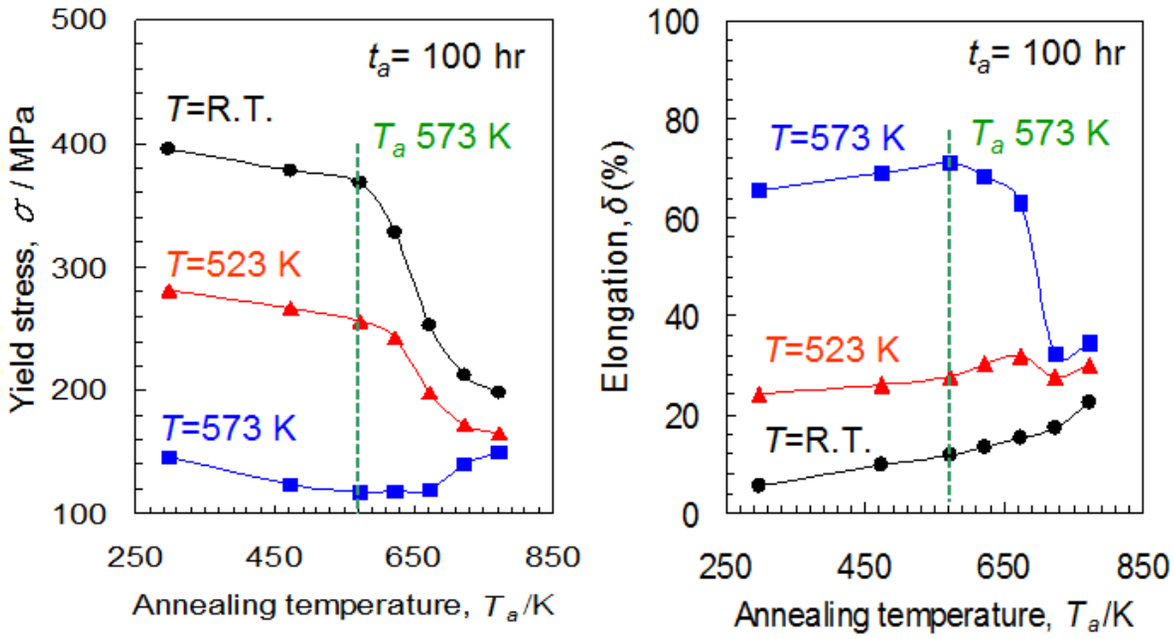


Figure 5. Mechanical properties of samples of $Mg_{96}Zn_2Y_2$ alloy extruded and annealed for 100 h at several temperatures. Tensile test were performed at room temperature to 573 K at an initial strain rate of 5.0×10^{-4} s^{-1}.

However, the dependence on the testing temperature was small in comparison with that of conventional Mg alloys [14]. In addition, the yield stress depended on the annealing temperature, but materials annealed at 573 K showed the same ratio as the yield stress of the as-extruded materials. There was a relative decrease in the yield stresses of materials annealed at a higher temperature of 673 K, regardless of the testing temperature. In this case, static recrystallization of the α-Mg phase and locally recovery and/or recrystallization of the LPSO phase of $Mg_{96}Zn_2Y_2$ alloy occur at 623 and 673 K, respectively. It is therefore important to maintain the kink band formed in the LPSO phase by extrusion to retain a high strength at high temperatures. When the tests were performed at 523 K, the yield stresses were 300 MPa for the as-extruded samples and 260 MPa for samples annealed at 623 K for 100 h. However, when the testing temperature was 573 K, the yield stress decreased to 120 MPa, regardless of the annealing temperature and time; however, the elongation showed a marked improvement to 70%. In other words the $Mg_{96}Zn_2Y_2$ alloy has excellent thermal stability and good mechanical properties for an annealing temperature of 573 K and a testing temperature of 523 K.

Figure 6 shows the effects of the annealing temperature and the annealing time on the mean recrystallized grain size of the α-Mg phase. The mean grain size of α-Mg phase increased

http://dx.doi.org/10.5772/48202

with increasing annealing temperature, but it remained only 20 μm, even after annealing for 100 h at 773 K, because the presence of the LPSO phase restrained the growth of grains of the α-Mg phase. Furthermore, the α-Mg phase showed grain growth for annealing times for 10 h, but increase in grain size was gradual even if the annealing time was extended to 100 h. The grain size of the α-Mg phase remained at 10 μm for an annealing temperature of 673 K, suggesting that the LPSO phase did recover or recrystallize locally, or that the microstructure was stable.

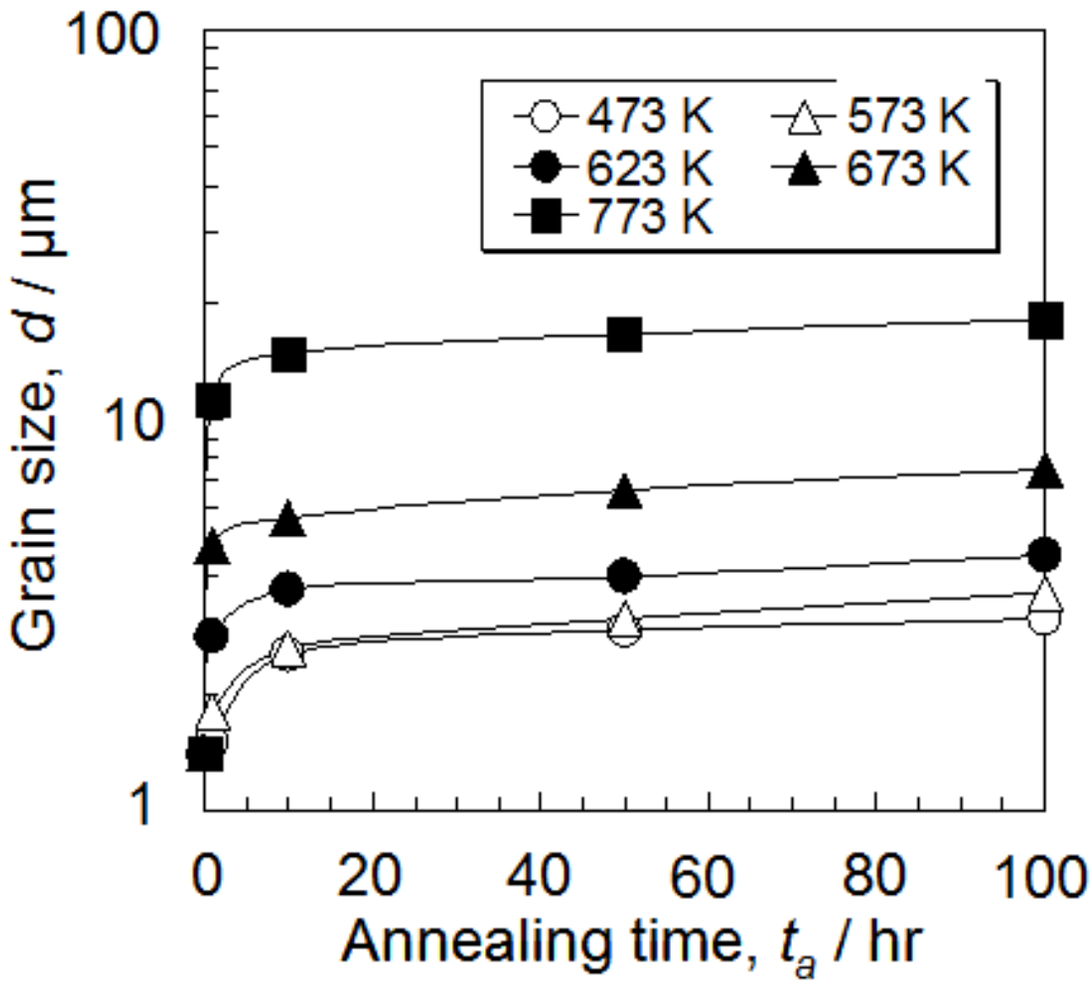


Figure 6. Relationship between the annealing conditions and the grain size of the α-Mg phase in samples of $Mg_{96}Zn_2Y_2$ alloy.

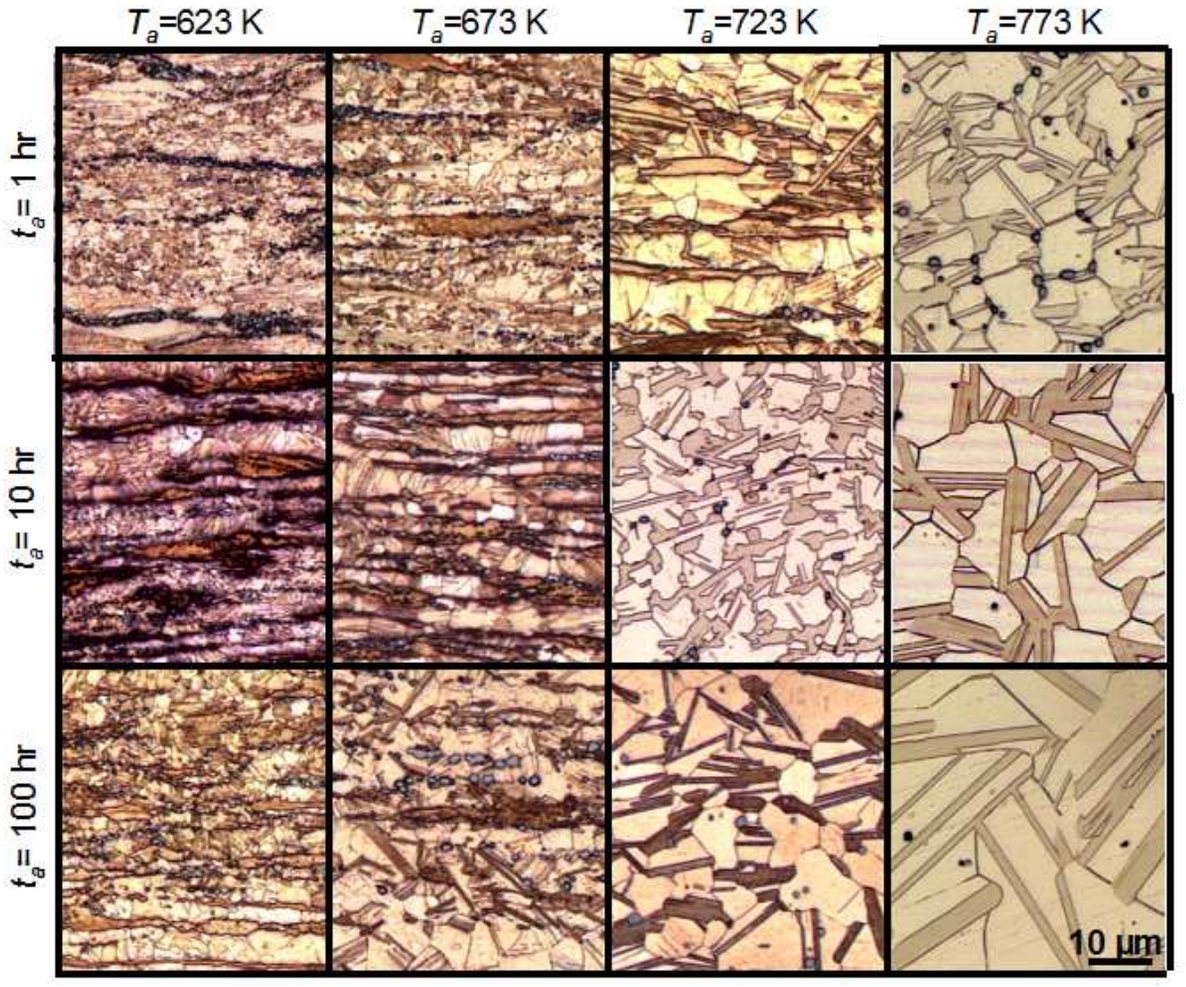


Figure 7. Optical micrographs of extruded samples of $Mg_{96}Zn_2Y_2$ alloy annealed at various temperatures for various holding times.

3.2. Microstructures of extruded and annealed samples of $Mg_{96}Zn_2Y_2$ alloy

Figure 7 shows optical micrographs of samples annealed at various temperatures and for various holding times. The average grain size of the α-Mg phase is shown in Figure 6. About 70% of the extruded $Mg_{96}Zn_2Y_2$ samples consisted of a recrystallized region and the remainder consisted of nonrecrystallized material. We suggest that discontinuous dynamic recrystallization occurs during extrusion. The grain size of the α-Mg phase increased on increasing the annealing temperature, but the grain size and the proportion of the recrystallized region did not change markedly at a temperature of 573 K. SEM micrographs of samples annealed at 623 K for 1 and 100 h are shown in Figure 8. The SEM micrographs show that, whereas the LPSO phase formed a block-type structure after annealing at 623 K for 1 h, a plate-type LPSO phase additionally appeared when the annealing time was extended to 100 h; the form of the LPSO phase therefore changed from a block type to a plate type when the annealing temperature was increased. Although annealing for about 1 h resulted only in local recovery or recrystallization of kink bands formed in the LPSO phase [10,15], an extension of

http://dx.doi.org/10.5772/48202

the annealing time permitted a change in form of the LPSO phase, even at 623 K. The formation of the plate-type LPSO phase from the block-type one is considered to result from redissolution and precipitation of the constituent elements.

SEM micrographs, TEM micrographs, IPF maps, and PF maps of samples annealed at 573 and 623 K for 100 h are shown in Figure 9. The SEM micrographs show that a plate-type LPSO phase appeared in samples annealed at 623 K for 100 h. The mean grain size of the α-Mg phase of materials annealed at 573 and 623 K were 3.4 and 4.8 μm, respectively, the intensities of texture were 6.1 and 3.0, respectively, and the proportions of recrystallized regions were 83 and 91%, respectively. The reason why the material annealed at 573 K show a high strength at room temperature and at high temperatures is that kink bands remain in the block-type LPSO phase and because the static recrystallization temperature of $Mg_{96}Zn_2Y_2$ alloy is higher than that shown by Mg alloys in general. As can be seen in Figure 9, the intensity of texture of samples annealed at 573 K for 100 h was similar to that of a rolled sheet of AZ31 Mg alloy subjected to working from 473 to 673 K until the rolling reduction reached 85.7%; the values were 7 and 5, respectively [16]. In other words, the presence of an LPSO phase containing kink bands is more important than are microstructural changes in the α-Mg phase. When the annealing temperature was increased to 673 K, the mean grain size of the α-Mg phase became 4.8 μm and kink bands showed a partial recovery, as observed by TEM studies on the microstructure (Figure 9). Figures 3–8 also show that significant changes occur in the mechanical properties and in the microstructure of $Mg_{96}Zn_2Y_2$ alloy during annealing at temperatures above 623 K. The recovery temperature for the LPSO phase is about 50 K higher than that of the α-Mg phase. It is important to note that formation of a kink band in the LPSO phase and microstructural refinement of the α-Mg phase during plastic deformation are responsible for the improvements in the mechanical properties of the alloy. In addition, we concluded that the alloy has superior strength and ductility because the LPSO phase constrains the growth grains in the α-Mg phase during annealing.

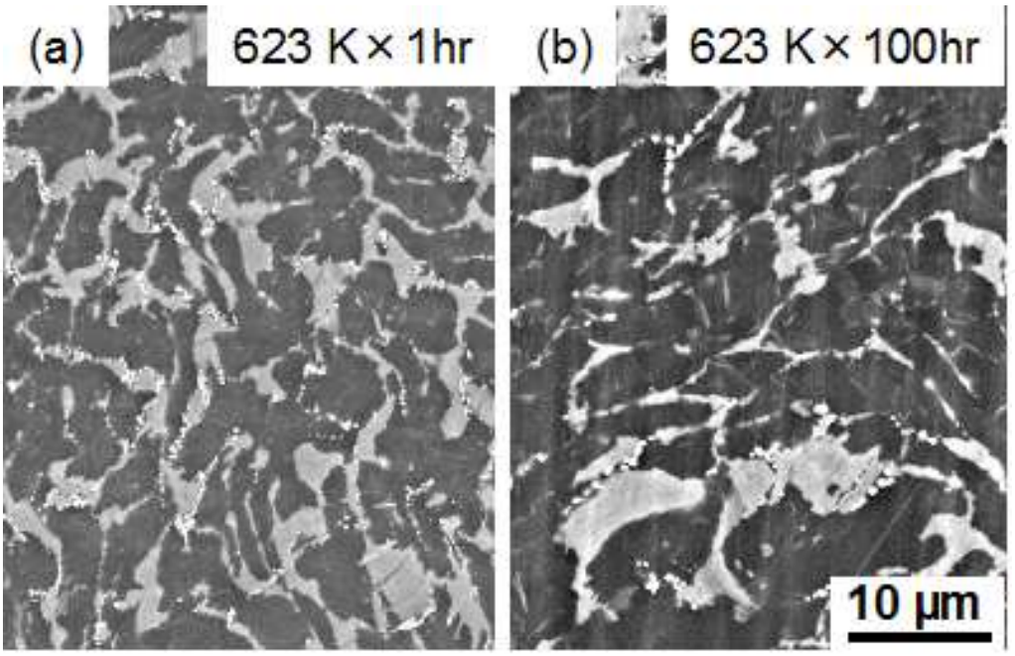


Figure 8. SEM micrographs of samples of $Mg_{96}Zn_2Y_2$ alloy annealed for (a) 623 K for 1 h and at (b) 623 K for 100 h.

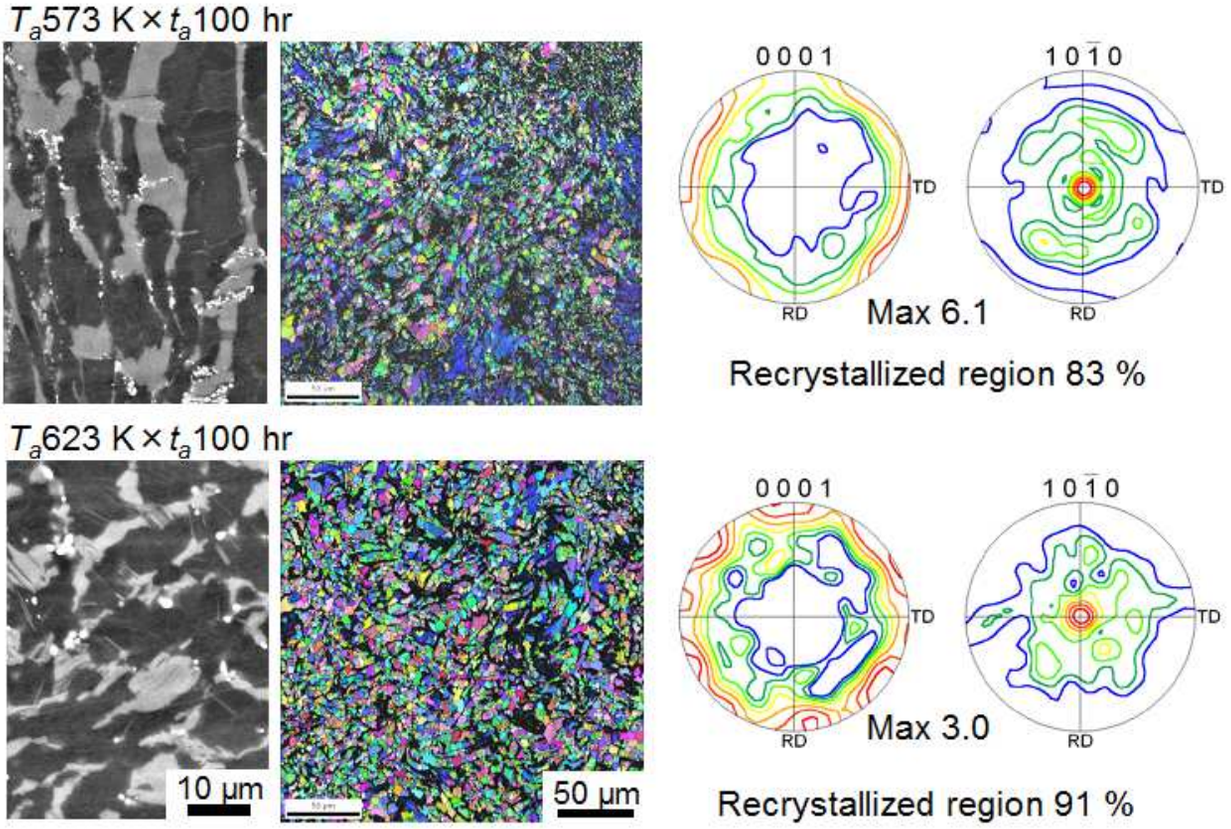


Figure 9. SEM micrographs, IPF maps, TEM micrographs, and PF maps of samples of $Mg_{96}Zn_2Y_2$ alloy annealed at 573 or 623 K for 100 h.

3.3. Thermal stability and the time–temperature–transformation diagram of extruded and annealed samples of $Mg_{96}Zn_2Y_2$

The extruded samples of $Mg_{96}Zn_2Y_2$ alloy did not shows any marked loss of strength or change in microstructure for annealing conditions of 573 K for 100 h and a testing temperature of 523 K. We therefore extended the annealing time to 1000 h to test the thermal stability of the alloy. Figure 10 shows the yield stress and elongation for a sample of extruded $Mg_{96}Zn_2Y_2$ alloy annealed at 573 K for various times up to 1000 h, as tested at room temperature and at 523 K. The yield stress and the tensile strength decreased gradually with increasing annealing time, whereas the elongation markedly improved. The tensile properties of samples annealed at 573 K for 1000 h did not depend on the annealing time or the testing temperature. Figure 11 shows SEM and TEM micrographs and an IPF map of a sample annealed at 573 K for 1000 h. Figure 10 shows that when the annealing temperature is maintained at 573 K for 1000 h, even though the yield stress is reduced from 391 to 352 MPa, the rates of decrease remain at 10 and 7%, respectively, and elongation is improved from 8 to 11%. Although the α-Mg phase grows from 1.5 μm to 4.8 μm, the LPSO phase forms a block-type structure, and a lamellar microstructure in which the LPSO phase is finely dispersed in the α-Mg phase forms; no substantial change was observed, even after annealing for 1000 h. In comparison with the TEM microstructure shown in Figure 11, where the sample was annealed for 1000 h, the LPSO phase is more bent and kink bands remain. The lamellar microstructure of the α-Mg and LPSO phases were the same as those observed before annealing.

The grains of the α-Mg phase coarsen as the annealing time is increased (see Figures 6 and 11). However, because the LPSO phase inhibits grain growth, the grain size is still fine compared with that of commercially available alloys. A crystallographic orientation analysis showed that 63% of the measured view for extruded materials and for materials annealed for 1 h consisted of high-angle grain boundaries and that the proportion of {10-10} crystalline orientation was 38%. However, because the grain size of the α-Mg phase increases with increasing annealing time, eventually 78% of the measured view consisted of high-angle grain boundaries and the proportion of {10-10} crystalline orientation fell to 11%. In other words, degradation of the mechanical properties of the extruded materials after annealing at 573 K is due to static recovery of the alloys. With regard to the reinforcing factor of this material, kink bands remained in the LPSO phase even after annealing at 573 K for 1000 h, and the LPSO phase formed a block-type structure. By the way, it is known that the LPSO phase is a harder material than the α-Mg phase. When an LPSO phase is present, the Mg alloy has a high strength and the grain growth of the α-Mg phase is constrained, but the microstructure remains unchanged. In the case of Mg alloys, it is important that they retain a high strength and a high ductility at high temperatures if they are to be used as industrial materials, and the LPSO-type Mg alloy is a material that can solve many such problems.

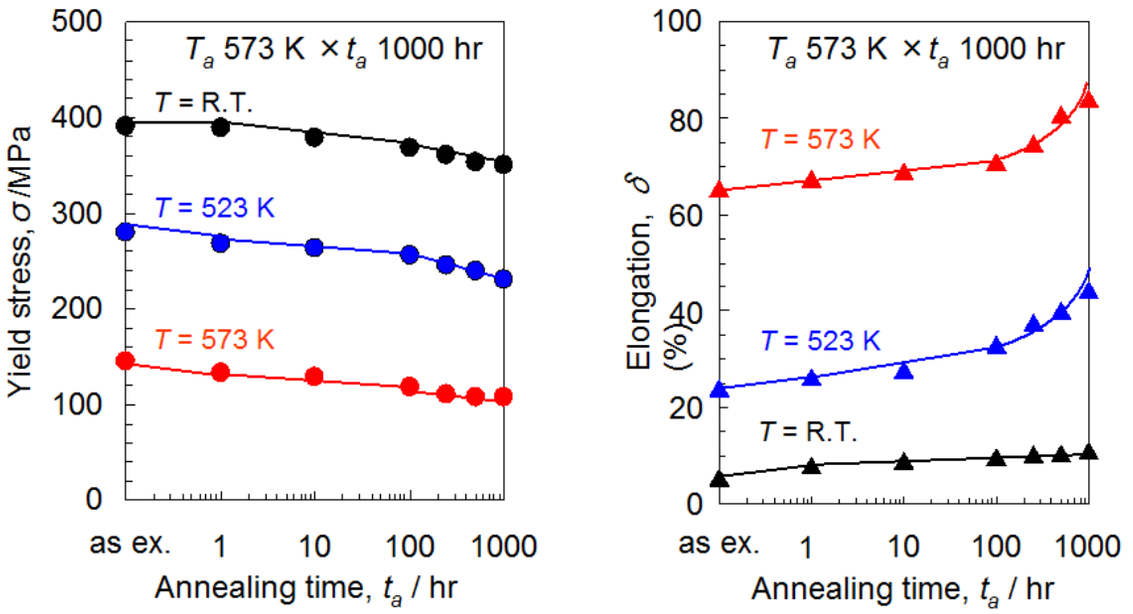


Figure 10. Relationship between the annealing time, mechanical properties, and testing temperatures for extruded samples of $Mg_{96}Zn_2Y_2$ alloy annealed at 573 K.

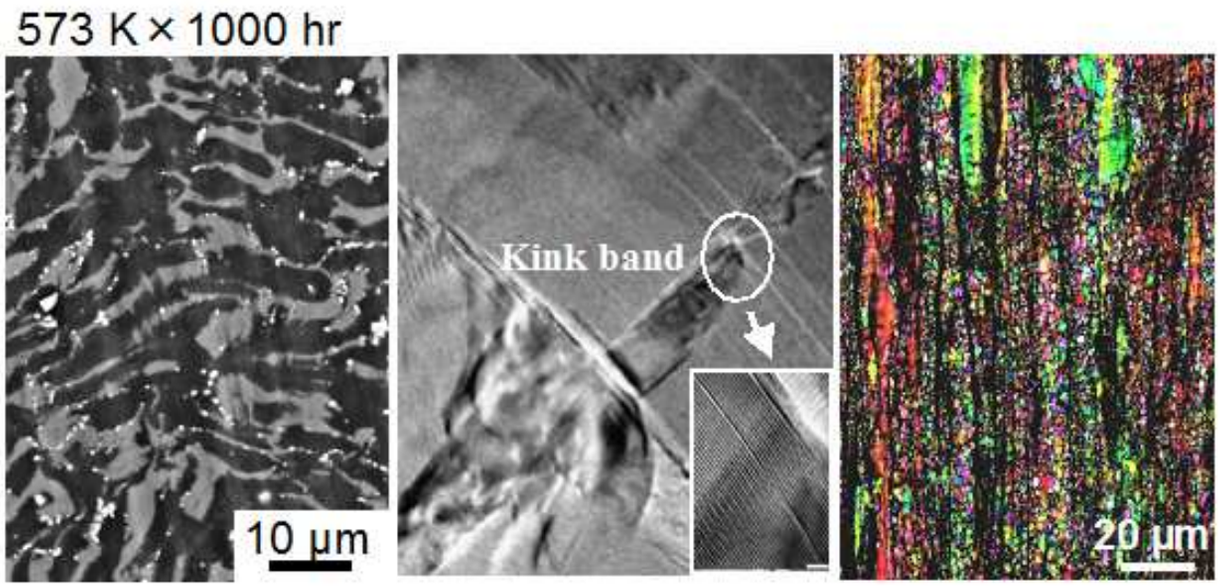


Figure 11. SEM and TEM micrographs and an IPF map of a sample of $Mg_{96}Zn_2Y_2$ alloy annealed at 573 K for 1000 h.

http://dx.doi.org/10.5772/48202

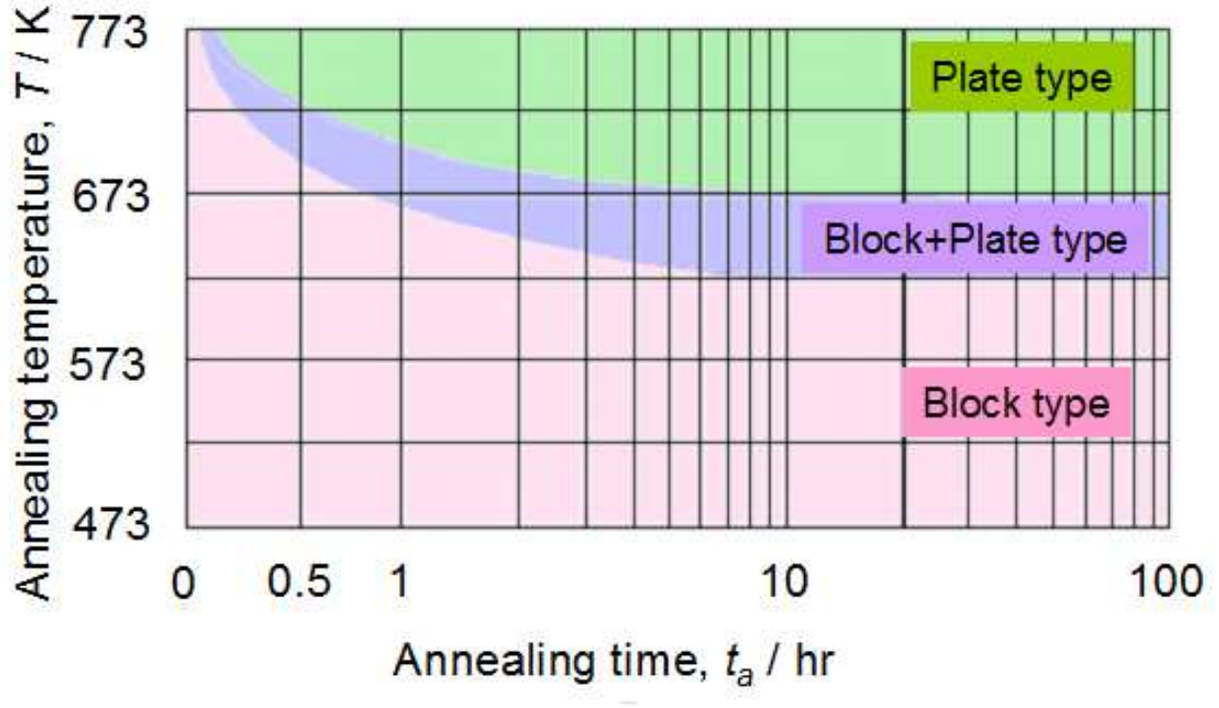


Figure 12. *TTT* diagram for extruded $Mg_{96}Zn_2Y_2$ alloy.

The time–temperature–transformation (*TTT*) diagram of $Mg_{96}Zn_2Y_2$ alloys (Figure 12), obtained by investigating the microstructure, strength, elongation, and thermal stability of as-extruded and annealed samples at room temperature and high temperatures, can be used to optimize working and forming processes. In Figure 12, the annealing temperature and annealing time graph is divided into three regions, depending on the shape of the LPSO phases: block type, block + plate type, or plate type. In the block-type region, annealing for a long time does not cause a marked deterioration in heat resistance or high strength. On the other hands, the plate-type region provides a high ductility, although the strength is reduced. We chose this classification in terms of the shape of LPSO phase because kink bands introduced into the LPSO phase play an important role in relation to the expression of high strength and high thermal stability of the $Mg_{96}Zn_2Y_2$ alloy.

3.4. Strength, microstructure, anisotropy, and rollability of samples of $Mg_{96}Zn_2Y_2$ alloy

Figure 13 shows SEM micrographs of an as-extruded sample of $Mg_{96}Zn_2Y_2$ alloy and of a sample annealed at 773 K for 1 h. The LPSO phase in the annealed materials appears to be more finely dispersed in a plate-type form than that in the extruded alloy. The volume fraction of the LPSO phase is similar to that of the as-extruded alloy, and a plate-type LPSO phase formed in several directions in the grains and grain boundaries. Normally, the LPSO phase, which is the secondary phase, acts as a fiber reinforcement and is anisotropic after plastic deformation. It has been reported [17] that in the as-extruded material, the yield stress in the direction of extrusion shows a difference of about 30% from that in the direction perpendicular to the extrusion direction. Here, the rolling process was performed in four

passes at 643 K with a roll temperature of 473 K. The samples were subsequently heated at 643 K for 5 min in an electric furnace and finally quenched in water. Table 1 shows the anisotropy of the tensile properties of hot-rolled sheets of the alloy, where an angle of 0° is parallel to the rolling direction. The maximum value of the anisotropy of the yield stress of the rolled material was about 10%, which is less than one third of that of the extruded material.

Tensile direction	YS (MPa)	UTS (MPa)	Elongation (%)
0°	365	410	5.5
45°	350	402	12
90°	328	398	7

Table 1. Relationship between the mechanical properties and the tensile direction for a rolled $Mg_{96}Zn_2Y_2$ sheet. The tensile test direction 0° was parallel to the direction of rolling.

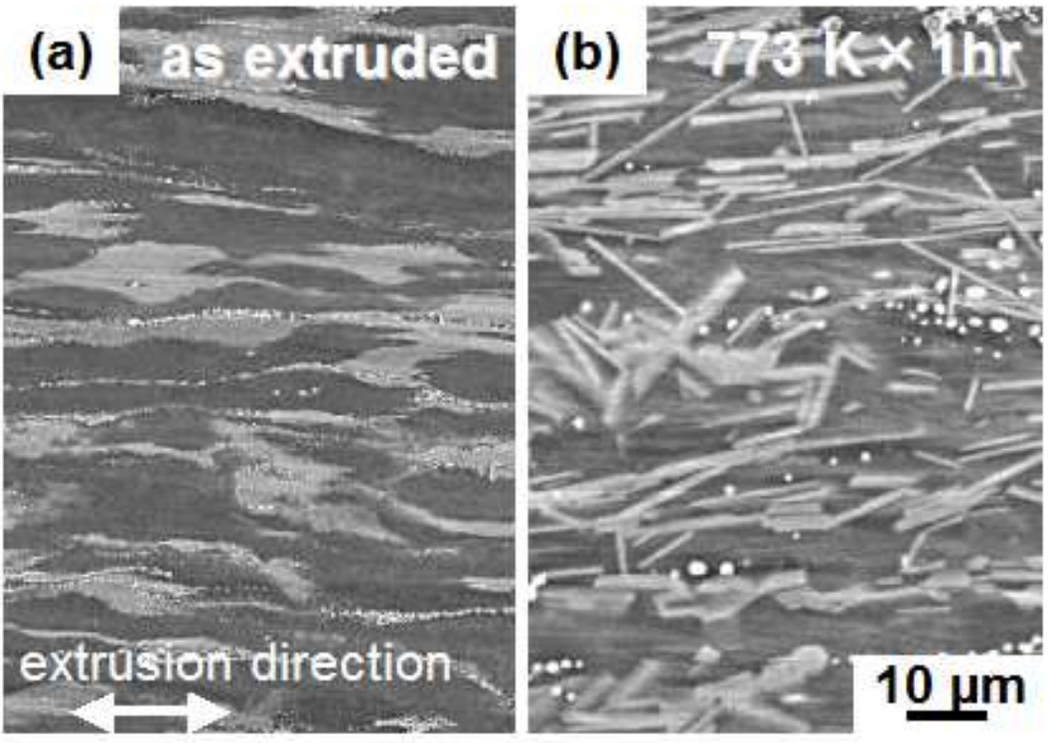


Figure 13. SEM micrographs of (a) as-extruded alloy $Mg_{96}Zn_2Y_2$ alloy and (b) a sample annealed at 773 K for 1 h.

The dispersal of the LPSO phase by heat treatment, as shown in Figure 13, is effective in reducing the anisotropy, and even low-deformation processing results in a high strength of over 360 MPa. The tensile strength was almost constant and was independent of the test direction. However, the elongation was maximal for a tensile direction of 45°. The LPSO phase is known to be a hard phase, but we were able to reduce the rolling processing temperature

http://dx.doi.org/10.5772/48202

by about 30 K and to perform the processing by using a schedule consisting of only a few passes. A four-pass schedule was the minimum number of passes for rolling the LPSO-type Mg alloy, and the strain ratio introduced by the rolling processing was 1.8, which is less than that produced by the extrusion process. However, the 0.2% proof stress and elongation of $Mg_{96}Zn_2Y_2$ rolled sheet material were 360 MPa and 5.5%, respectively. In other words, the Mg alloy regained its high strength even when its LPSO phase was not subject to severe plastic deformation.

Optical micrographs and IPF maps are show in Figures 14 and 15, respectively. In Figure 14, the darker regions correspond to the LPSO phase. The LPSO phase has a large curvature in the rolling direction and shows considerable deformation. Furthermore, the formation of kink bands can be recognized in the LPSO phase. Normally, the LPSO phase does not show a large curvature in extruded materials, and we suggest that the large deformation of the LPSO phase observed in this case is responsible for the development of high strength by the rolling process. From Figure 15, we estimated that the grain size of the α-Mg phase in the rolled material was 5.0 μm. The intensity of texture of rolled sheet was 4.9, which is low in comparison with that of as-rolled AZ31 Mg alloy. Fine grains (mean size <5.0 μm) were formed around the LPSO phase, and it is possible that stress concentration acts on the α-Mg phase, because the LPSO phase is bent in the rolling process, causing dynamic recrystallization. The frequencies of low-angle and high-angle grain boundaries in the $Mg_{96}Zn_2Y_2$ rolled sheet were 19.3% and 80.7%, respectively. The rolling process is therefore capable of producing a high frequency of high-angle grain boundaries and a random crystal orientation in $Mg_{96}Zn_2Y_2$ alloy.

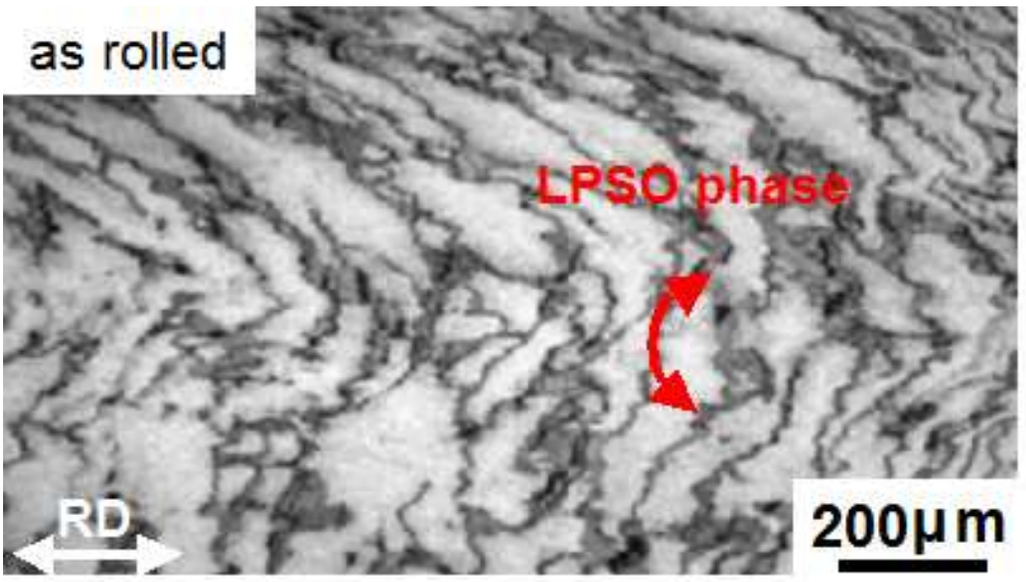


Figure 14. Optical micrograph of as-rolled $Mg_{96}Zn_2Y_2$ alloy.

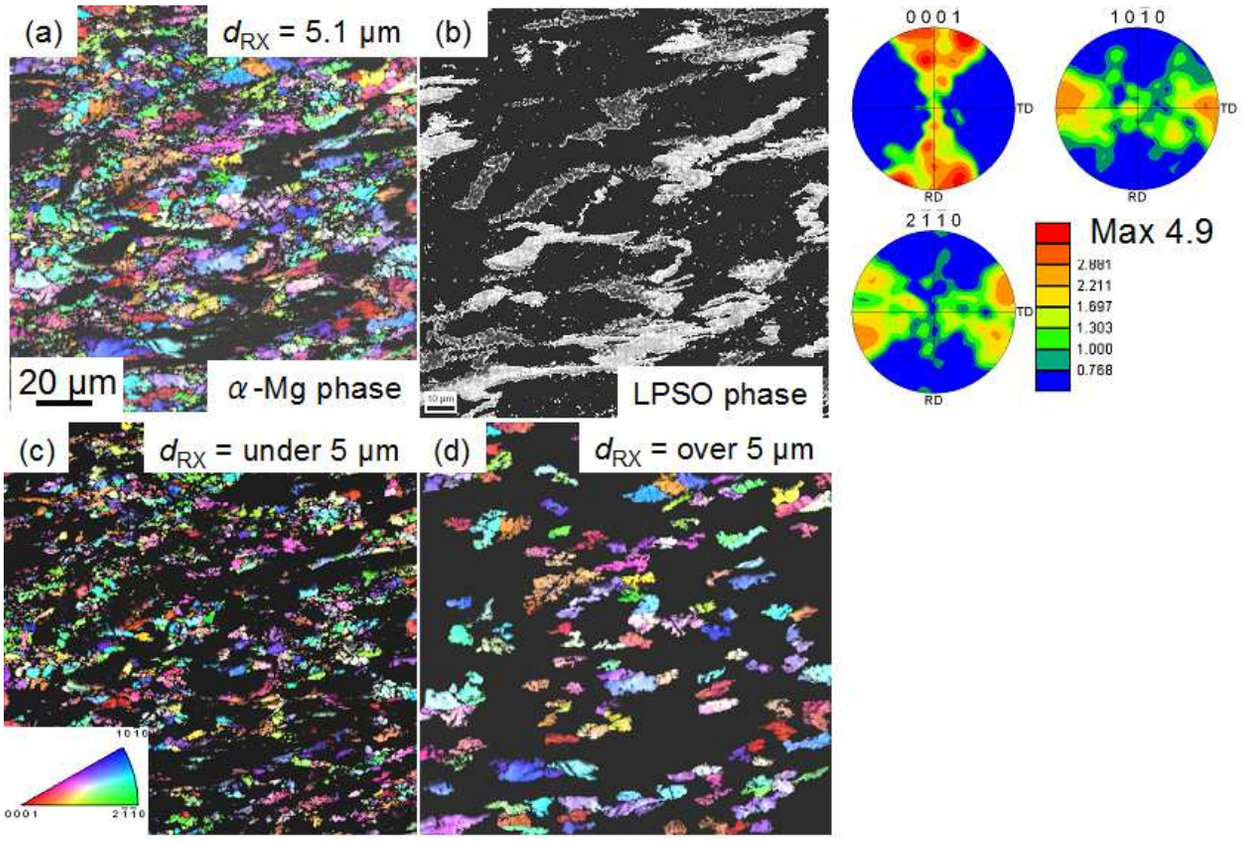


Figure 15. IPF and PF maps of as-rolled $Mg_{96}Zn_2Y_2$ alloy; the intensity of texture is indicated in the PF maps. Figures (c) and (d) were cropped from the IPF map; (c) shows the fine-grain region and (d) shows the coarse-grain region.

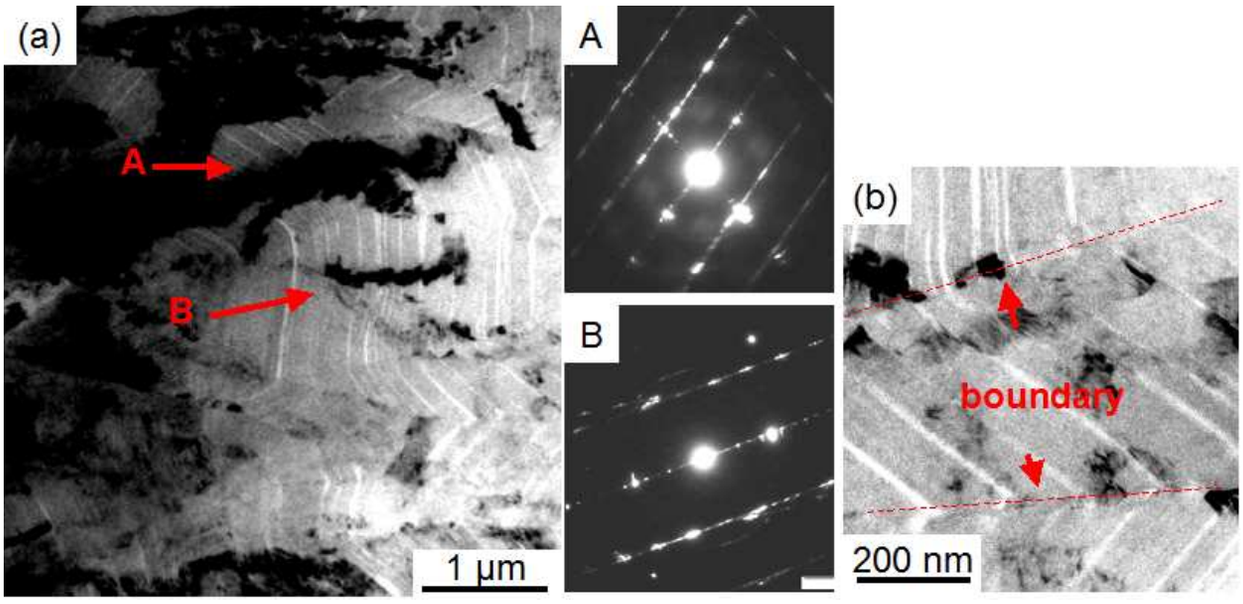


Figure 16. TEM micrographs of the as-rolled $Mg_{96}Zn_2Y_2$ alloy; (b) is high-magnification image of a kink boundaries.

http://dx.doi.org/10.5772/48202

TEM micrographs of the LPSO phases in an as-rolled sheet of $Mg_{96}Zn_2Y_2$ alloy are shown in Figure 16. In the rolled sheet, the LPSO phase was continuously deformed, but boundaries were observed in some regions, suggested that the LPSO phase recovered, at least partially, from the kink deformation introduced during rolling process. Although it is difficult to compare results of a previous study [18] directly with those of the present study, for FCC metals, cellular microstructures at the boundary between the deformation band and the deformation matrix act as recovery nuclei during subsequent reheating. We assume that the kinks acted as recovery nuclei in the $Mg_{96}Zn_2Y_2$ alloy and led to the formation of a static structure when edge dislocations accumulated as a result of reheating of the kink deformation that formed within the LPSO phase. In the $Mg_{96}Zn_2Y_2$ rolled sheet, the LPSO phase was continuously deformed, but boundaries were observed in some regions, suggesting that the LPSO phase recovered, at least partially, from the kink deformation introduced during the hot-rolling process. The present study clarified that continuous deformation of kink bands is necessary to permit the LPSO phase to show large deformations and that recovery of kink bands during reheating is important.

4. Conclusions

The mechanical properties and microstructures of extruded $Mg_{96}Zn_2Y_2$ alloys annealed at various temperatures with various holding times were investigated. Annealing the extruded $Mg_{96}Zn_2Y_2$ alloy at 623 K caused reductions in yield stress and a gradual decrease in the tensile strength; however, the ductility improved from 5.4 to 9.6%. The α-Mg phase and LPSO phase showed static recrystallization and recovery at 623 and 673 K, respectively; therefore the $Mg_{96}Zn_2Y_2$ alloy showed a superior thermal stability when it was annealed at 573 K. An effective way to improve the ductility of the alloy while maintaining high strength involves ensuring recovery of the secondary LPSO phase from kink bands, controlling the grain size of the α-Mg phase, and producing a fine dispersion of the LPSO phase in the α-Mg phases. In hot-rolled samples of $Mg_{96}Zn_2Y_2$ alloy, the anisotropy of the rolled sheet alloy was low compared with that of the extruded alloy when rolling was performed at 673 K after annealing treatment. The important factors in the development of $Mg_{96}Zn_2Y_2$ alloy with a high strength and ductility are a fine dispersion of the LPSO phase in the grain boundary and the formation of continuous kink bands and/or boundary in the LPSO phase.

Acknowledgement

The authors are grateful for the financial supports from the Kumamoto Prefecture Collaboration of Regional Entities supported this work for the Advancement of Technological Excellence, Japan Science and Technology Agency. The examination of rolling process went by the furtherance from Grant-in-Aid for Young Scientists for (B) No. 23760099 from Japan Society for the Promotion of Science.

Author details

Masafumi Noda[1*], Kunio Funami[1], Yoshihito Kawamura[2] and Tsuyoshi Mayama[2]

Department of Mechanical Science and Engineering, Chiba Institute of Technology, Tsudanuma, Narashino, Chiba,, Japan

Department of Material Science, Kumamoto University, Kurokami, Kumamoto,, Japan

References

[1] Alan, A., & Luo, . (2003). Recent Magnesium Alloy Development for Automotive Powertrain Applications. Materials Science Forum 419-422: 57-66.

[2] M.H. Yoo (1981). Slip, Twinning, and Fracture in Hexagonal Close-Packed Metals. Metallurgical Transactions A 12A: ., 409-418.

[3] Ion, S. E., Humphreys, F. J., & White, S. H. (1982). Dynamic Recrystallisation and the Development of Microstructure During the High Temperature Deformation of Magnesium. Acta Metallurgica , 30, 1909-1919.

[4] Watanabe, H., & Ishikawa, K. (2009). Effect of Texture on High Temperature Deformation Behavior at High Strain Rates in a Mg-3Al-1Zn Alloy. Mater. Sci. Eng. A ., 523, 304-311.

[5] Kawamura, Y., Hayashi, K., Inoue, A., & Masumoto, T. (2001). Rapidly Solidified Powder Metallurgy Mg97Zn1Y2 Alloys with Excellent Tensile Yield Strength Above 600 MPa. Materials Transactions ., 42, 1172-1176.

[6] Kawamura, Y., & Yamasaki, M. (2007). Formation and Mechanical Properties of Mg97Zn1RE2 Alloys with Long Period Stacking Ordered Structure. Materials Transactions ., 48, 2986-2992.

[7] Yoshimoto, S., Yamasaki, M., & Kawamura, Y. (2006). Microstructure and Mechanical Properties of Extruded Mg-Zn-Y Alloys with 14H Long Period Ordered Structure. Materials Transactions ., 47, 959-965.

[8] Itoi, T., Inazawa, T., Kuroda, Y., Yamasaki, M., Kawamura, Y., & Hirohashi, M. (2010). Tensile property and cold formability of a Mg96Zn2Y2 alloy sheet with a long-period ordered phase. Materials Letters ., 64, 2277-2280.

[9] Matsumoto, R., Yamasaki, M., Otsu, M., & Kawamura, Y. (2009). Forgeability and Flow Stress of Mg-Zn-Y Alloys with Long Period Stacking Ordered Structure at Elevated Temperatures. Materials Transactions ., 50, 841-846.

http://dx.doi.org/10.5772/48202

[10] Noda, M., Mayama, T., & Kawamura, Y. (2009). Evolution of Mechanical Properties and Microstructure in Extruded Mg96Zn2Y2 Alloys by Annealing. Mater. Trans. ., 50, 2526-2531.

[11] Stanford, N. (2010). Micro-Alloying Mg with Y, Ce, Gd and La for Texture Modification- A Comparative Study. Materials Science and Engineering A ., 527, 2669-2677.

[12] Barnett, M. R., Keshavarz, Z., Beer, A. G., & Atwell, D. (2004). Influence of Grain Size on the Compressive Deformation of Wrought Mg-3Al-1Zn. Acta Materialia ., 52, 5093-5103.

[13] Su, C. W., Lu, L., & Lai, M. O. (2007). Mechanical Behavior and Texture of Annealed AZ31 Mg Alloy Deformed by ECAP. Materials Science and Technology ., 23, 290-296.

[14] Kim, W. J., Chung, S. W., Chung, C. S., & Kum, D. (2001). Superplasticity in Thin Magnesium Alloy Sheets and Deformation Mechanism Maps for Magnesium Alloys at Elevated Temperatures. Acta Materialia ., 49, 3337-3345.

[15] Myshlyaev, M. M., Mc Queen, H. J., Mwembela, A., & Konopleva, E. (2002). Twinning, Dynamic Recovery and Recrystallization in Hot Worked Mg-Al-Zn Alloy. Materials Science and Engineering A ., 337, 121-133.

[16] Chino, Y., Mabuchi, M., Kisihara, R., Hosokawa, H., Yamada, Y., Wen, C., Shimojima, K., & Iwasaki, H. (2002). Mechanical Properties and Press Formability at Room Temperature of AZ31 Mg Alloy Processed by Single Roller Drive Rolling. Material Transactions ., 43, 2554-2560.

[17] Mayama, T., Noda, M., Kawamura, Y., & Hagihara, K. (2009). Anisotropic Compressive Behavior of Extruded Magnesium Alloy Mg96Zn2Y2: Experimental Observation and Crystal Plasticity Analysis. Collected extended abstracts of Thermec 2009: 302.

[18] Higashida, K., Takamura, J., & Narita, N. (1986). The Formation of Deformation Bands in F.C.C. Crystals. Materials Science and Engineering ., 81, 239-258.

IntechOpen

IntechOpen